Convolution quadrature boundary element method for quasi-static visco- and poroelastic continua

Martin Schanz *, Heinz Antes, Thomas Rüberg

Institute of Applied Mechanics, Technical University Braunschweig, P.O. Box 3329, D-38023 Braunschweig, Germany

Abstract

The main difference of convolution quadrature method (CQM)-based boundary element formulations to usual time-stepping BE formulations is the way to solve the convolution integral appearing in most time-dependent integral equations. In the CQM formulation, the convolution integrals are approximated by a quadrature rule whose weights are determined by the Laplace transformed fundamental solutions and a multi-step method. So, there is no need of a time domain fundamental solution. For quasi-static problems in visco- or poroelasticity time-dependent fundamental solutions are available, but these fundamental solutions are highly complicated yielding to very sensitive algorithms. Especially in viscoelasticity, for every rheological model a separate fundamental solution must be deduced.

Here, firstly, viscoelastic as well as poroelastic constitutive equations are recalled and, then, the respective integral equations are presented. Applying the usual spatial discretization and using the CQM for the temporal discretization yields the final time-stepping algorithm. The proposed methodology is tested by two simple examples considering creep behavior in viscoelasticity and consolidation processes in poroelasticity. The algorithm shows no stability problems and behaves well over a broad range of time step sizes.
© 2004 Elsevier Ltd. All rights reserved.

Keywords: Quasi-static viscoelasticity; Quasi-static poroelasticity; Biot's theory; Convolution quadrature method; BEM

1. Introduction

Convolution quadrature method (CQM)-based boundary element (BE) formulations are first published in 1997 [1,2] with applications in elasto- or viscoelastodynamics. The main difference to usual time-stepping BE formulations is the way to solve the convolution integral appearing in most time-dependent integral equations. In the CQM formulation, this convolution integral is approximated by a quadrature rule whose weights are determined by the Laplace transformed

fundamental solutions and a multi-step method [3,4]. An overview of this BE formulation is given in [5].

There are mainly two reasons to use a CQM-based BEM instead of usual time-stepping procedures. One reason is to improve the stability of the time-stepping procedure [1,6]. The other reason is to tackle problems where no time-dependent fundamental solutions are available, e.g., for inelastic material behavior in viscoelastodynamics [7], in poroelastodynamics [8], or for functional graded materials [9]. Also, this method is used to avoid highly complicated fundamental solutions in time domain [10–12].

However, up to now, the CQM-based BEM is used only in dynamic formulations. Clearly, for quasi-static

* Corresponding author. Fax: +49 531 391 5843.
E-mail address: m.schanz@tu-bs.de (M. Schanz).

problems as in visco- or poroelasticity there is no need to apply the CQM because time-dependent fundamental solutions are available, e.g., for viscoelasticity in [13,14] and for poroelasticity in [15]. However, these fundamental solutions are highly complicated yielding to very sensitive algorithms and, especially in viscoelasticity [16], for every rheological model a separate fundamental solution must be deduced, which is even not possible for very complicated rheological models. Therefore, it is promising to apply the CQM also to the quasi-static integral equations in visco- and poroelasticity.

Here, at first, viscoelastic as well as poroelastic constitutive equations are recalled whereas in viscoelasticity a generalized 3-parameter model (see, e.g., [17]) serves as an example and Biot's theory [18] is used in poroelasticity. It should be mentioned that the proposed method can also be applied on mixture theory based theories as the Theory of Porous Media [19] because the mathematical operator of the governing equations is equal to that of Biot's theory, as shown for the dynamic case by Schanz and Diebels [20]. For both constitutive assumptions, viscoelasticity and poroelasticity, the fundamental solutions in Laplace domain are given and the singular behavior is discussed. For viscoelasticity such solutions are found by applying the elastic–viscoelastic correspondence principle [21] to the elastostatic fundamental solutions. In case of poroelasticity, the quasi-static fundamental solutions in Laplace domain may be found in [22] or in the survey article by Cheng and Detournay [23].

Subsequent to the formulation of the constitutive and governing equations, the respective integral equations are presented. Applying the usual spatial discretization and using the CQM for the temporal discretization yields the final time-stepping algorithm. Concerning the treatment of the singular integrals, the well known procedures from elasticity can be used because the singular parts of the integrals are equal to the elastic case. Finally, the proposed methodology is tested with simple examples for creep behavior in viscoelasticity or for consolidation processes in poroelasticity.

Throughout this paper, the summation convention is applied over repeated indices and Latin indices receive the values $1, 2$, and $1, 2, 3$ in two-dimensions (2-d) and three-dimensions (3-d), respectively. Commas $(\ )_{,i}$ denote spatial derivatives and, as usual, the Kronecker delta is denoted by δ_{ij}.

2. Governing equations and fundamental solutions

In the following, the constitutive equations and the governing equations for a viscoelastic continuum and a poroelastic continuum are given in a short form. The intention is only to point out the notation and to state the basic assumptions. For a more detailed description on viscoelasticity the reader is referred to [21] and on poroelasticity to Biot's original work [18] or to the quite comprehensive article of Detournay and Cheng [24]. Further, as the convolution quadrature method uses fundamental solutions only in Laplace domain, it is sufficient to give the governing equations and their fundamental solutions in Laplace domain.

2.1. Quasi-static viscoelasticity

Decomposing the stress tensor σ_{ij} and strain tensor ϵ_{ij} into their hydrostatic parts $\delta_{ij}\sigma_{kk}/3$, $\delta_{ij}\epsilon_{kk}/3$ and the deviatoric parts s_{ij}, e_{ij} and assuming a linear isothermal viscoelastic material, e.g., a generalized three parameter model, two independent sets of constitutive equations exist in the Laplace domain

$$\left(1 + p^D s^{\alpha^D}\right)\hat{s}_{ij} = 2G\hat{e}_{ij}\left(1 + q^D s^{\alpha^D}\right) \tag{1a}$$

$$\left(1 + p^H s^{\alpha^H}\right)\hat{\sigma}_{kk} = \frac{2G(1+v)}{1-2v}\hat{\epsilon}_{kk}\left(1 + q^H s^{\alpha^H}\right), \tag{1b}$$

when $\hat{f}(s)$ denotes the Laplace transform of a function $f(t)$ with the complex Laplace variable s. In the Eq. (1), the shear modulus G and the Poisson's ratio v are used as elastic material constants . The index H or D indicates that the constitutive parameters p, q and the fractional power α can be different for the hydrostatic part H and the deviatoric part D of the stress–strain relation.

A plausible model of the viscoelastic phenomenon should predict non-negative internal work, a non-negative rate of energy dissipation [25], and finite wave velocities. Therefore, the parameters are constrained by [26]

$$0 \leqslant p^D < q^D; \quad 0 < \alpha^D < 2; \quad 0 \leqslant p^H < q^H;$$
$$0 < \alpha^H < 2. \tag{2}$$

Comparing the viscoelastic constitutive equation (1) with Hooke's law, the elastic–viscoelastic correspondence principle $G \Longleftrightarrow G(s)$ and $v \Longleftrightarrow v(s)$ is obtained with

$$G(s) = G\frac{1 + q^D s^{\alpha^D}}{1 + p^D s^{\alpha^D}}$$
$$v(s) = \frac{(1+v)\left(1 + q^H s^{\alpha^H}\right)\left(1 + p^D s^{\alpha^D}\right) - (1-2v)\left(1 + q^D s^{\alpha^D}\right)\left(1 + p^H s^{\alpha^H}\right)}{2(1+v)(1 + q^H s^{\alpha^H})(1 + p^D s^{\alpha^D}) + (1-2v)(1 + q^D s^{\alpha^D})(1 + p^H s^{\alpha^H})}, \tag{3}$$

where G and v without the argument (s) denote the elastic material data whereas $G(s)$ and $v(s)$ means the complex moduli from viscoelasticity. Hence, every elastodynamic solution of a specific problem can be converted to the solution of the related viscoelastic problem by replacing the elastic material data by the complex moduli (3) [21].

In Eq. (3), the dependence of Poisson's ratio $v(s)$ from the Laplace parameter s is clearly observed, which corresponds to a time-dependent Poisson's ratio. If, however, the parameters satisfy the relation

$$\left(1 + q^H s^{\alpha^H}\right)\left(1 + p^D s^{\alpha^D}\right) = \left(1 + q^D s^{\alpha^D}\right)\left(1 + p^H s^{\alpha^H}\right),$$
(4)

which means that the deviatoric part and the hydrostatic part of the stress–strain relation behave similar, Poisson's ratio is also for viscoelasticity no function of s, i.e., time invariant, and equal to the elastic case [21].

Inserting the viscoelastic constitutive equation (1) in the static equilibrium $\sigma_{ij,j} = -f_i$ yields the governing equation in Laplace domain

$$G(s)\hat{u}_{i,jj}(\mathbf{x},s) + \frac{G(s)}{(1 - 2v(s))}\hat{u}_{j,ij}(\mathbf{x},s) = -\hat{f}_i(\mathbf{x},s).$$
(5)

This is the viscoelastic equivalent to the Lamé field equations where the only difference is the dependence of the material parameters on the Laplace variable s. Clearly, this equation can be obtained by applying the elastic–viscoelastic correspondence principle on the elastic Lamé equations. Since both, the displacements $\hat{u}_i$ and the material factors are dependent on s, the inverse transformation yields an integrodifferential equation as governing equation in time domain. Due to this, solutions in time domain are very rare. However, via the elastic–viscoelastic correspondence principle in Laplace domain, with a subsequent inverse Laplace transform, solutions of several problems may be found.

Here, the fundamental solution is required for the BE formulation. Fortunately, the CQM based BE formulation uses only the Laplace transformed fundamental solution which is easily achieved with the elastic–viscoelastic correspondence principle. So, the displacement fundamental solution for a quasi-static viscoelastic continuum is

$$\widehat{U}_{ij} = \frac{1}{16\pi G(s)r(1 - v(s))}\left\{r_{,i}r_{,j} + \delta_{ij}(3 - 4v(s))\right\}$$
(6)

and the corresponding traction fundamental solution is

$$\widehat{T}_{ij} = \frac{-1}{8\pi(1 - v(s))r^2}\left\{\left[(1 - 2v(s))\delta_{ij} + 3r_{,i}r_{,j}\right]r_{,n} - (1 - 2v(s))\left(r_{,j}n_i - r_{,i}n_j\right)\right\}.$$
(7)

The dependence on $r = |\mathbf{x} - \mathbf{y}|$, i.e., the distance between field and load point, is the same as for the elastostatic fundamental solutions. So, the displacement

fundamental solution is weakly singular and the traction fundamental solution strongly singular. Obviously, the same procedures as in elastostatics to tackle these singularities can be applied. However, it should be mentioned that the singular part of the traction fundamental solution is in viscoelasticity dependent on s, i.e., time-dependent. Only for the special case of (4), the traction fundamental solution (7) is equal to the elastostatic one and, therefore, not dependent on s.

2.2. Quasi-static poroelasticity

Following Biot's approach to model the behavior of porous media, the constitutive equations can be expressed as

$$\sigma_{ij} = G(u_{i,j} + u_{j,i}) + \left(K - \frac{2}{3}G\right)\delta_{ij}u_{k,k} - \alpha\delta_{ij}p$$

and

$$\zeta = \alpha u_{k,k} + \frac{1}{M}p$$
(8)

in which σ_{ij} denotes the total stress, p the pore pressure, u_i the displacements of the solid frame, and ζ the variation of fluid volume per unit reference volume. The sign convention for stress and strain follows that of elasticity, namely, tensile stress and strain is denoted positive. The bulk material is defined by the shear modulus G and the compression modulus K, known from elasticity. The porosity ϕ, Biot's effective stress coefficient α, and M complete the set of material parameters. Further, a linear strain-displacement relation $\varepsilon_{ij} = 1/2(u_{i,j} + u_{j,i})$ is used, i.e., small deformation gradients are assumed.

Conservation of the linear momentum yields the static equilibrium

$$\sigma_{ij,j} = -F_i$$
(9)

formulated for the mixture, i.e., for the solid and the interstitial fluid. In Eq. (9), F_i denotes the bulk body forces. The mass conservation is governed by the continuity equation

$$\frac{\partial}{\partial t}\zeta + q_{i,i} = a,$$
(10)

with the specific flux of the fluid q_i and a source term $a(t)$. Finally, the interstitial flow is modeled with Darcy's law

$$q_i = -\kappa p_{,i}$$
(11)

where κ denotes the permeability.

As shown in [27], it is sufficient to use the solid displacement and the pore pressure as basic variables to describe a poroelastic continuum. Therefore, the above equations are reduced to these four unknowns. Clearly, contrary to the dynamic case, this can be achieved even in time domain by eliminating the flux in the above given equations. However, because in the following only the

Laplace transformed equations are necessary, Eqs. (8)–(11) are transformed to Laplace domain. Subsequently, eliminating the flux yields the final set of differential equations for the displacements $\hat{u}_i$ and the pore pressure $\hat{p}$

$$G\hat{u}_{i,jj} + \left(K + \frac{1}{3}G\right)\hat{u}_{j,ij} - \alpha\hat{p}_{,i} = -\hat{F}_i \quad (12a)$$

$$\kappa\hat{p}_{,ii} - \frac{s}{M}\hat{p} - \alpha s\hat{u}_{i,i} = -\hat{a}. \quad (12b)$$

It must be mentioned that vanishing initial conditions for all state variables are assumed.

The fundamental solutions for the system of governing Eq. (12) are solutions due to single forces in the solid in all three spatial directions $\hat{F}_i\mathbf{e}_j = \delta(\mathbf{x} - \mathbf{y})\delta_{ij}$ denoted by $\hat{U}_{ij}^s$ and $\hat{P}_i^s$ as well due to a single source in the fluid $\hat{a} = \delta(\mathbf{x} - \mathbf{y})$ denoted by $\hat{U}_i^f$ and $\hat{P}^f$, i.e., in total four functions. These solutions can be found in the literature, e.g., in [22], and are given for convenience in Appendix A. For developing a BE formulation the corresponding integral equation to the system (12) is used where an essential feature is the singular behavior of the fundamental solutions and their derivatives, i.e., the flux and the traction fundamental solution. Simple series expansion with respect to the variable $r = |\mathbf{x} - \mathbf{y}|$ shows that these solutions behave in the limit $r \to 0$ like the elastic or the acoustic fundamental solutions, i.e., in 3-d

$$\hat{U}_{ij}^s = \frac{1}{16\pi Gr(1-v)}\{r_{,i}r_{,j} + \delta_{ij}(3 - 4v)\} + O(r^0) \quad (13a)$$

$$\hat{P}^f = \frac{1}{4\pi\kappa}\frac{1}{r} + O(r^0) \quad (13b)$$

$$\hat{T}_{ij}^s = \frac{-1}{8\pi(1-v)r^2}\left\{\left[(1-2v)\delta_{ij} + 3r_{,i}r_{,j}\right]r_{,n} - (1-2v)(r_{,j}n_i - r_{,i}n_j)\right\} + O(r^0) \quad (13c)$$

$$\hat{T}_i^f = \frac{s\alpha(1-2v)}{8\pi\kappa(1-v)}\frac{1}{r}[n_i + r_{,i}r_{,n}] + O(r^0) \quad (13d)$$

$$\hat{Q}_j^s = \frac{\alpha(1-2v)}{16\pi(1-v)}\frac{1}{r}[r_{,j}r_{,n} - n_j] + O(r^0) \quad (13e)$$

$$\hat{Q}^f = -\frac{1}{4\pi}\frac{r_{,n}}{r^2} + O(r^0). \quad (13f)$$

In Eq. (13), $r_{,n} = r_{,k}n_k$ denotes the normal derivative and the fundamental solutions $\hat{U}_i^f = s\hat{P}_i^s = O(r^0)$ are regular.

3. Quasi-static boundary element formulation

To establish a BE formulation an integral equation corresponding to the governing equations must be derived. For both constitutive assumptions, viscoelasticity

and poroelasticity, the usual methods, i.e., weighted residuals or reciprocal work theorem, can be used. Here, the corresponding integral equations are only recalled where a derivation for viscoelasticity may be found in [28] and for poroelasticity in [29].

So, starting from a weighted residual statement defined on the domain Ω with boundary Γ using fundamental solutions as weighting functions an integral equation is achieved. Next, performing two partial integrations with respect to the spatial variable yields the boundary integral equations. With careful regard to the singular behavior of the fundamental solutions, the load point $\mathbf{y}$ is shifted to the boundary. Based on the governing Eq. (5), the integral equation for viscoelasticity

$$c_{ij}(\mathbf{y}, t) * u_i(\mathbf{y}, t) = \int_\Gamma U_{ij}(\mathbf{x}, \mathbf{y}, t) * t_i(\mathbf{x}, t)\mathrm{d}\Gamma - \oint_\Gamma T_{ij}(\mathbf{x}, \mathbf{y}, t) * u_i(\mathbf{x}, t)\mathrm{d}\Gamma \quad (14)$$

and based on the poroelastic system of Eq. (12), the respective integral equations for poroelasticity

$$\begin{bmatrix} c_{ij}(\mathbf{y}) & 0 \\ 0 & c(\mathbf{y}) \end{bmatrix}\begin{bmatrix} u_i(t, \mathbf{y}) \\ p(t, \mathbf{y}) \end{bmatrix}$$
$$= \int_\Gamma \begin{bmatrix} U_{ij}^s(t, \mathbf{y}, \mathbf{x}) & -P_j^s(t, \mathbf{y}, \mathbf{x}) \\ U_i^f(t, \mathbf{y}, \mathbf{x}) & -P^f(t, \mathbf{y}, \mathbf{x}) \end{bmatrix} * \begin{bmatrix} t_i(t, \mathbf{x}) \\ q(t, \mathbf{x}) \end{bmatrix}\mathrm{d}\Gamma$$
$$- \oint_\Gamma \begin{bmatrix} T_{ij}^s(t, \mathbf{y}, \mathbf{x}) & Q_j^s(t, \mathbf{y}, \mathbf{x}) \\ T_i^f(t, \mathbf{y}, \mathbf{x}) & Q^f(t, \mathbf{y}, \mathbf{x}) \end{bmatrix} * \begin{bmatrix} u_i(t, \mathbf{x}) \\ p(t, \mathbf{x}) \end{bmatrix}\mathrm{d}\Gamma. \quad (15)$$

are achieved. The time domain representation is obtained by a formal inverse Laplace transform where all products between two Laplace parameter dependent functions are transformed into convolution integrals

$$f * g = \int_0^t f(t - \tau)g(\tau)\mathrm{d}\tau. \quad (16)$$

The integral free terms c_{ij} and c are due to the strongly singular behavior of the last integrals in (14) and (15) where $\oint_\Gamma$ denotes the Cauchy principal value of the integral. As seen from the singular parts of the traction fundamental solutions (7) and (13c), the integral free terms c_{ij} differ only in the time-dependency of the viscoelastic case compared to the constant term in the poroelastic case. But, finally, both are equal to elastostatics with respect to the spatial behavior. The integral free term c is equal to acoustics which can be seen from Eq. (13f). So, the procedure proposed by Mantič [30] to determine these terms can be used.

Next, a boundary element formulation is achieved following the usual procedure, i.e., introducing spatial and temporal discretization. For simplicity this procedure is only described for the more complex poroelastic

integral equation (15) which includes the single integral equation of viscoelasticity (14). Differences in both formulations are remarked.

3.1. Spatial discretization

First, the boundary surface Γ is discretized by E isoparametric elements Γ_e where F polynomial shape functions $N_e^f(\mathbf{x})$ are defined. Hence, the following ansatz functions with the time-dependent nodal values $u_i^{ef}(t)$, $t_i^{ef}(t)$, $p^{ef}(t)$, and $q^{ef}(t)$ are used to approximate the boundary states

$$
\begin{aligned}
u_i(\mathbf{x},t) &= \sum_{e=1}^{E}\sum_{f=1}^{F} N_e^f(\mathbf{x})u_i^{ef}(t),\\
t_i(\mathbf{x},t) &= \sum_{e=1}^{E}\sum_{f=1}^{F} N_e^f(\mathbf{x})t_i^{ef}(t),\\
p(\mathbf{x},t) &= \sum_{e=1}^{E}\sum_{f=1}^{F} N_e^f(\mathbf{x})p^{ef}(t),\\
q(\mathbf{x},t) &= \sum_{e=1}^{E}\sum_{f=1}^{F} N_e^f(\mathbf{x})q^{ef}(t).
\end{aligned}
\tag{17}
$$

In Eq. (17), the shape functions of all four variables are denoted by the same function $N_e^f(\mathbf{x})$ indicating the same approximation level for all variables. This is not mandatory but usual. Clearly, in viscoelasticity, ansatz functions have to be chosen only for the displacements and tractions. Inserting these ansatz functions (17) in the time-dependent integral Eq. (15) yields

$$
\begin{aligned}
&\begin{bmatrix} c_{ij}(\mathbf{y}) & 0 \\ 0 & c(\mathbf{y}) \end{bmatrix}\begin{bmatrix} u_i(\mathbf{y},t) \\ p(\mathbf{y},t) \end{bmatrix}\\
&= \sum_{e=1}^{E}\sum_{f=1}^{F}\left\{\int_{\Gamma}\begin{bmatrix} U_{ij}^s(r,t) & -P_j^s(r,t) \\ U_i^f(r,t) & -P^f(r,t) \end{bmatrix}\right.\\
&\quad\times N_e^f(\mathbf{x})\mathrm{d}\Gamma * \begin{bmatrix} t_i^{ef}(t) \\ q^{ef}(t) \end{bmatrix} - \oint_{\Gamma}\begin{bmatrix} T_{ij}^s(r,t) & Q_j^s(r,t) \\ T_i^f(r,t) & Q^f(r,t) \end{bmatrix}\\
&\quad\left.\times N_e^f(\mathbf{x})\mathrm{d}\Gamma * \begin{bmatrix} u_i^{ef}(t) \\ p^{ef}(t) \end{bmatrix}\right\}.
\end{aligned}
\tag{18}
$$

3.2. Temporal discretization

Next, a time discretization has to be introduced. Instead of using the time-dependent fundamental solutions, here, the convolution quadrature method (briefly summarized in Appendix B) is used as a promising alternative.

Hence, after dividing time period t in N time steps of equal duration Δt, so that $t = N\Delta t$, the convolution integrals between the fundamental solutions and the nodal values in (18) are approximated by the convolution quadrature method, i.e., the quadrature formula (B.1)

is applied to the integral Eq. (18). This results in the following boundary element time-stepping procedure $(n = 0, 1, \ldots, N)$

$$
\begin{aligned}
&\begin{bmatrix} c_{ij}(\mathbf{y}) & 0 \\ 0 & c(\mathbf{y}) \end{bmatrix}\begin{bmatrix} u_i(\mathbf{y},n\Delta t) \\ p(\mathbf{y},n\Delta t) \end{bmatrix}\\
&= \sum_{e=1}^{E}\sum_{f=1}^{F}\sum_{k=0}^{n}\left\{\begin{bmatrix} \omega_{n-k}^{ef}\left(\widehat{U}_{ij}^s,\mathbf{y},\Delta t\right) & -\omega_{n-k}^{ef}\left(\widehat{P}_j^s,\mathbf{y},\Delta t\right) \\ \omega_{n-k}^{ef}\left(\widehat{U}_i^f,\mathbf{y}\Delta t\right) & -\omega_{n-k}^{ef}\left(\widehat{P}^f,\mathbf{y}\Delta t\right) \end{bmatrix}\right.\\
&\quad\times\begin{bmatrix} t_i^{ef}(k\Delta t) \\ q^{ef}(k\Delta t) \end{bmatrix} - \begin{bmatrix} \omega_{n-k}^{ef}\left(\widehat{T}_{ij}^s,\mathbf{y},\Delta t\right) & \omega_{n-k}^{ef}\left(\widehat{Q}_j^s,\mathbf{y},\Delta t\right) \\ \omega_{n-k}^{ef}\left(\widehat{T}_i^f,\mathbf{y},\Delta t\right) & \omega_{n-k}^{ef}\left(\widehat{Q}^f,\mathbf{y},\Delta tq\right) \end{bmatrix}\\
&\quad\left.\times\begin{bmatrix} u_i^{ef}(k\Delta t) \\ p^{ef}(k\Delta t) \end{bmatrix}\right\}
\end{aligned}
\tag{19}
$$

with the integration weights corresponding to (B.3), e.g., (for details see Appendix B)

$$
\begin{aligned}
&\omega_n^{ef}\left(\widehat{U}_{ij}^s,\mathbf{y},\Delta t\right)\\
&= \frac{\mathscr{R}^{-n}}{L}\sum_{\ell=0}^{L-1}\int_{\Gamma}\widehat{U}_{ij}^s\left(\mathbf{x},\mathbf{y},\frac{\gamma\left(\mathscr{R}\mathrm{e}^{\mathrm{i}\ell\frac{2\pi}{L}}\right)}{\Delta t}\right)N_e^f(\mathbf{x})\mathrm{d}\Gamma\mathrm{e}^{-\mathrm{i}n\ell\frac{2\pi}{L}}.
\end{aligned}
\tag{20}
$$

Note, the calculation of the integration weights is only based on the Laplace transformed fundamental solutions. Therefore, with this time-stepping procedure (19), a boundary element formulation for quasi-static poroelasticity is given without time-dependent fundamental solutions. The same is true for the quasi-static viscoelastic BE formulation

$$
\begin{aligned}
&\sum_{k=0}^{n}\omega_{n-k}(\hat{c}_{ij},\mathbf{y},\Delta t)u_i(\mathbf{y},k\Delta t)\\
&= \sum_{e=1}^{E}\sum_{f=1}^{F}\sum_{k=0}^{n}\left\{\omega_{n-k}\left(\widehat{U}_{ij},\mathbf{y},\Delta t\right)t_i^{ef}(k\Delta t)\right.\\
&\quad\left.-\omega_{n-k}\left(\widehat{T}_{ij},\mathbf{y},\Delta t\right)u_i^{ef}(k\Delta t)\right\}
\end{aligned}
\tag{21}
$$

where, contrary to the formulation (19), also the convolution of the integral free term must be considered. However, as remarked above, for the case of similar viscoelastic behavior of the hydrostatic and deviatoric constitutive assumption, i.e., Eq. (4) is fulfilled, the summation on the left hand side of Eq. (21) vanishes.

To calculate the integration weights ω_{n-k}^{ef} in (19) and (21), spatial integration over the boundary Γ has to be performed. The regular integrals are evaluated by standard Gaussian quadrature rule and the weakly singular parts of the integrals in (19) and (21) are regularized by polar coordinate transformation. The strongly singular integrals in (19) and (21) are equal to those of elastostatics or acoustics, respectively, and, hence, the regularization methods known from these theories can be applied,

e.g., the method suggested by Guiggiani and Gigante [31]. Moreover, to obtain a system of algebraic equations, collocation is used at every node of the shape functions $N_e^f(\mathbf{x})$.

According to $t - \tau = (n - k)\Delta t$, the integration weights ω_{n-k}^{ef} are only dependent on the difference $n - k$. This property is analogous to elastodynamic time domain BE formulations (see, e.g., [32]) and can be used to establish a recursion formula for $n = 1, 2, \ldots, N$ ($m = n - k$)

$$\omega_0(\mathbf{C})\mathbf{d}^n = \omega_0(\mathbf{D})\bar{\mathbf{d}}^n + \sum_{m=1}^{n} (\omega_m(\mathbf{U})\mathbf{t}^{n-m} - \omega_m(\mathbf{T})\mathbf{u}^{n-m}).$$

(22)

with the time-dependent integration weights ω_m containing the Laplace transformed fundamental solutions. Similarly, $\omega_0(\mathbf{C})$ and $\omega_0(\mathbf{D})$ are the corresponding integration weights of the first time step related to the unknown boundary data $\mathbf{d}^n$ and the known boundary data $\bar{\mathbf{d}}^n$ in the time step n, respectively. Finally, a direct equation solver is applied.

4. Example: creeping and consolidation

To show the accuracy and the robustness of the proposed formulation, the displacement response of a 3-d bar is calculated using a viscoelastic constitutive law as well as using a poroelastic constitutive law. The material data are given in Table 1. In the case of viscoelasticity, the material data of a perspex (PMMA) are used based on experiments performed at the Institute of Technical Mechanics, Technical University Braunschweig. In the case of poroelasticity, the soil material data are taken from literature [33].

First, tests on the influence of mesh size and time step size are presented and, subsequently, the creep behavior of the perspex bar and the consolidation of a soil half space close this example section.

4.1. Influence of mesh and time step size

To study the influence of the mesh and the time step size on the proposed BE formulation, a 3-d bar (3 m × 1 m × 1 m) is considered. This bar is fixed at one
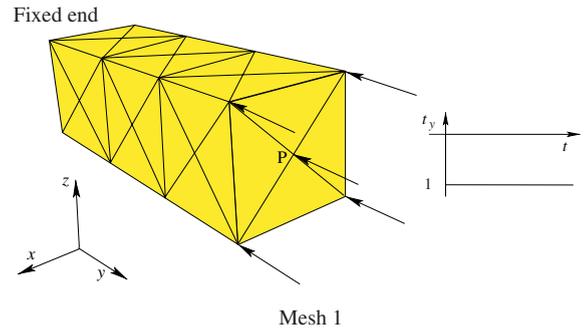

Fig. 1. Geometry, loading, and discretization (mesh 1) of the 3-d bar.

end and loaded with $t_y = -1 \, \text{N/m}^2 H(t)$ over the whole time period on the other end. The remaining surface is modeled traction free for the viscoelastic test. Whereas for the poroelastic test, the normal displacements are blocked and in tangential directions free sliding, i.e., zero traction, is modeled. Further, the free surface where the load as total stress function is applied is assumed to be permeable, i.e., the prescribed pore pressure vanishes. All other surfaces including the fixed end are impermeable, i.e., the flux vanishes there. The geometry, the coarsest mesh (mesh 1), and the time history of the load are shown in Fig. 1.

The mesh 1 (see Fig. 1) consists of 56 linear elements on 38 nodes. Additionally, three finer meshes are used for a numerical convergence study: In the Fig. 2, mesh 2 with 112 linear elements on 102 nodes, mesh 3 with 324 linear elements on 188 nodes, and mesh 3 with 700 linear elements on 392 nodes are shown. In Fig. 3, the calculated displacements at point P (the middle point of the free and loaded surface) are plotted versus time for the viscoelastic case and for the poroelastic case. These results are compared with analytical 1-d solutions. For the viscoelastic bar the analytical solution is obtained by applying the elastic–viscoelastic correspondence principle on the elastostatic solution. A subsequent inverse Laplace transform yields the displacement at the free end

$$u_{\text{visco}}(y = 3 \, \text{m}) = \frac{t_y 3}{E}\left(1 - e^{-t/q}\left(1 - \frac{p}{q}\right)\right).$$

(23)

Table 1
Material data of perspex (PMMA) and a soil (coarse sand)

Poroelastic (soil)					
K (N/m²)	ϕ	G (N/m²)	α	M (N/m²)	κ (m⁴/Ns)
2.1×10^8	0.48	9.8×10^7	0.980918	5.24×10^9	3.55×10^{-9}

Viscoelastic (PMMA)							
G (N/m²)	v	p^H (s⁻¹)	q^H(s⁻¹)	α^H	p^D(s⁻¹)	q^D(s⁻¹)	α^D

(a) Mesh 2   **(b)** Mesh 3

(c) Mesh 4
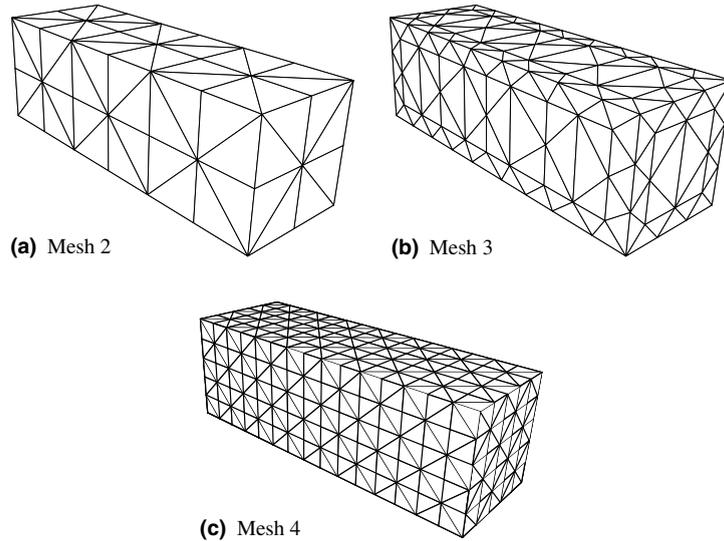
Fig. 2. Discretization steps of the 3-d bar.

(a) Viscoelasticity

(b) Poroelasticity
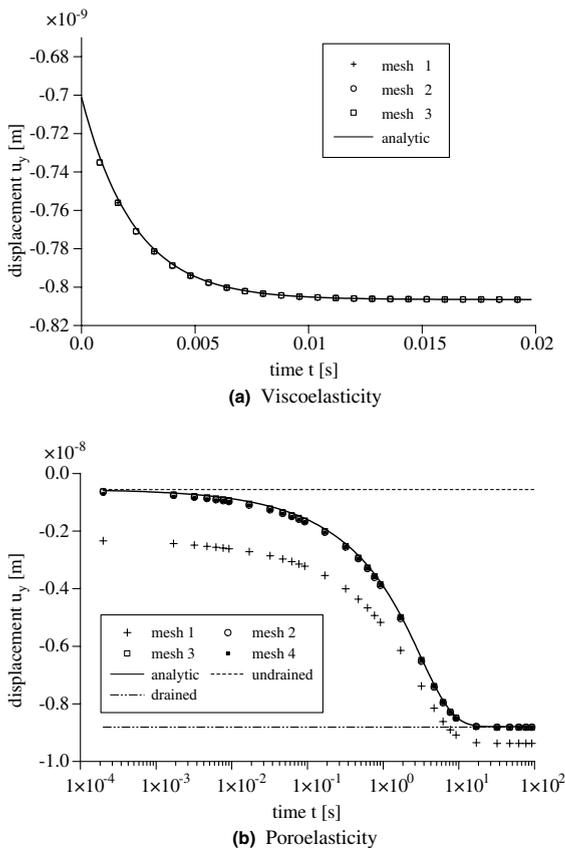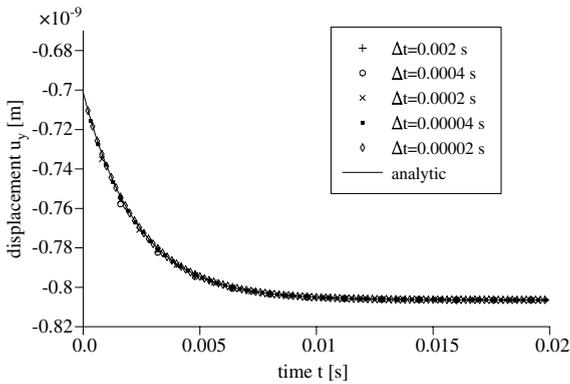
Fig. 3. Displacement at the free end versus time: different mesh results compared to the analytical solution.

The poroelastic analytical 1-d solution is taken from the literature [24].

In the case of viscoelasticity, the results for meshes 1–3 are presented showing a perfect agreement of all three discretization with the analytical solution. It can be concluded that even the coarse mesh 1 is sufficient. Contrary, in case of the poroelastic formulation mesh 1 is not sufficient. Only the results of the finer meshes 2–4 coincide whereas for the results of mesh 1 only the tendency is acceptable. For comparison also the limiting cases of an undrained elastic bar and a drained elastic bar are given. As expected, in the short time range, the poroelastic results coincide with the undrained elastostatic solution and in the long time range the drained elastostatic solution is obtained. It can be concluded that the poroelastic formulation needs a much finer spatial discretization than the viscoelastic formulation which is in agreement with the experiences of the corresponding dynamic formulation [5].

Comparing now the sensitivity of the proposed formulations with respect to the time step size Δt, a complete different situation is observed. In Fig. 4, the displacements versus time are presented but now using different time step sizes and mesh 1 for the viscoelastic results and mesh 3 for the poroelastic results, respectively. The time step size is varied from $\Delta t = 0.002$ to $\Delta t = 0.00002$ s in case of viscoelasticity and from $\Delta t = 1$ to $\Delta t = 0.01$ s in case of poroelasticity, i.e., in both cases by a factor of 100. There is a perfect coincidence of the different graphs for the different time step sizes, respectively, indicating that the proposed formulation is not influenced by the chosen time step size. In case of poroelasticity, however, the time step $\Delta t = 1$ s is not able to resolve the early time response ($t < 4$ s) well. Further, not presented numerical studies with larger as well as smaller time step sizes as used here,

(a) Viscoelasticity
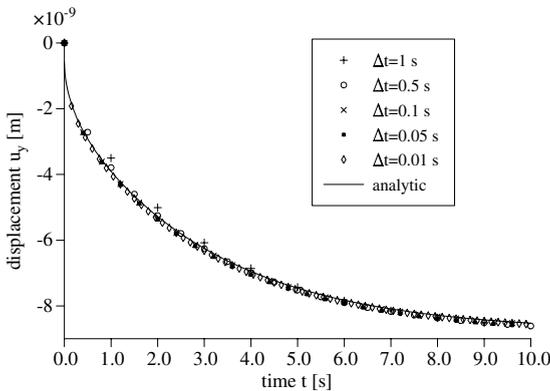
(b) Poroelasticity

Fig. 4. Displacement at the free end versus time: influence of different time step sizes.

are performed confirming the above observation. Clearly, for resolving small times a small time step size is required, however, this is not caused by the proposed formulation but by the physical process to be described. So, it can be concluded that the given formulation is not influenced by the chosen time step size.

A final test to show the accuracy of the proposed method is the pressure distribution in the bar. In Fig. 5, the pore pressure is depicted versus the position of y along the midline of the bar. The BE results are compared with the analytical 1-d solution [24] at three different times. For $t = 1$ and $t = 10$ s a perfect agreement is found. At smaller times, $t = 0.1$ s, slight deviations from the analytical solution are visible close to the fixed end. But, because the field of applications of quasi-static poroelasticity is mainly the analysis of consolidation problems, i.e., of long time studies, these deviations are no problem.

4.2. Viscoelastic creep behavior

Among other effects in viscoelasticity, the creeping behavior is expected. To show this effect in Fig. 6, again
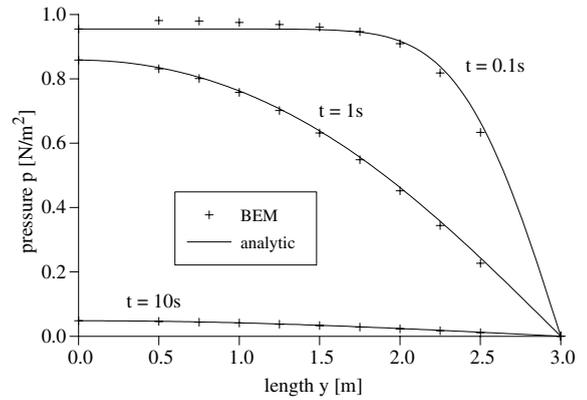

Fig. 5. Pressure distribution along the midline of the poroelastic bar at different times.

the displacement at point P is depicted versus time. Additionally, two elastostatic responses are given as straight lines: one calculated with the initial modulus $G(t = 0) = Gq^H/p^H$ and the other with the long time modulus $G(t \to \infty) = G$. Note, the 3-d bar is loaded by a negative stress vector, i.e., a pressure load, so that the viscoelastic result creeps 'negative'. It can be expected from theory that the viscoelastic response starts at the elastostatic result for $G(t = 0)$ and approximates the elastostatic result for $G(t \to \infty)$. In Fig. 6, this expected behavior can be clearly observed showing that the proposed formulation reproduces the physical background correctly.

4.3. Poroelastic consolidation

In quasi-static poroelasticity, the main interest is in calculating the consolidation of the poroelastic material.
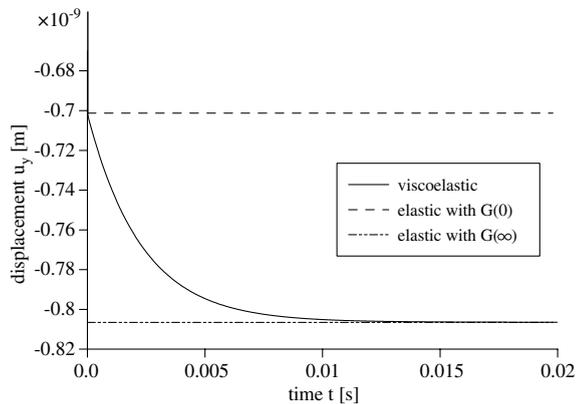

Fig. 6. Displacement at the free end: creeping behavior of a perspex bar.
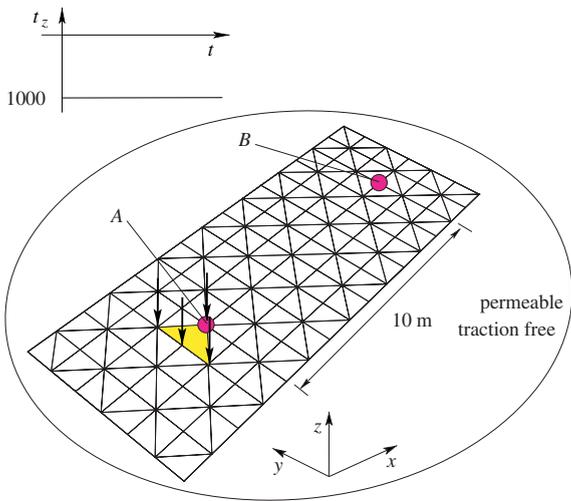
Fig. 7. Poroelastic half space: geometry, mesh, and load.

To simulate this behavior, a poroelastic half space is modeled as sketched in Fig. 7. The mesh is truncated outside an area of $6\,\text{m} \times 15\,\text{m}$ and the material data are those of soil (see Table 1). The load perpendicular to the surface is modeled by the total stress vector $t_z = -1000\,\text{N/m}^2\,H(t)$ on the shaded area (near point A) and kept constant over time. The remaining surface is traction free and permeable, i.e., the pore pressure is assumed to be zero at the surface.

In Fig. 8, the displacements on the surface at point A and at point B are depicted versus time. Note, in Fig. 8(a) the short time behavior (20 s) is presented whereas in Fig. 8(b) the long time behavior (12 h) is shown. In both cases, the consolidation process is obvious where this process is faster below the load than in 10 m distance from the load at point B.

Additionally to the settlement, the pore pressure distribution below the surface is of interest. In Fig. 9, the pore pressure is depicted versus depth for four different times, i.e., at $t = 0.1$, $t = 0.5$, $t = 1$, and $t = 5$ s. As before, not only at point A below the load (Fig. 9(a)) but also at
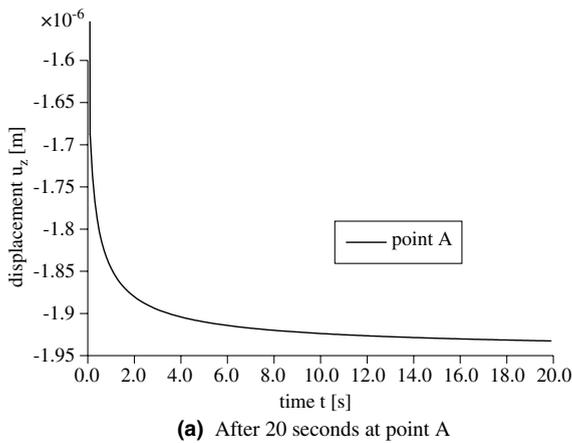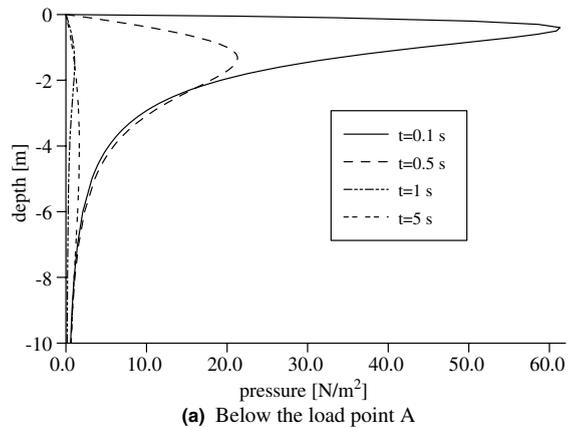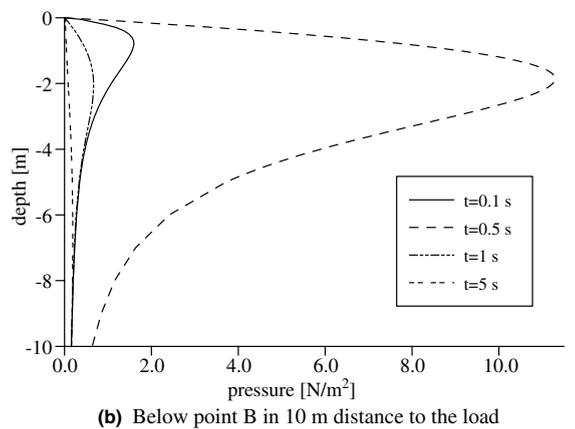

(a) After 20 seconds at point A
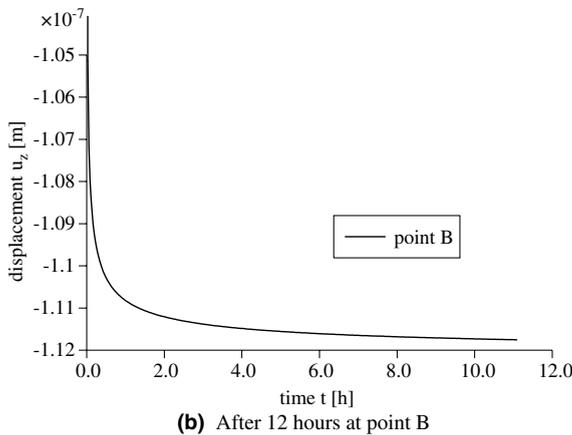
(b) After 12 hours at point B

Fig. 8. Surface displacement versus time for different time scales.

(a) Below the load point A

(b) Below point B in 10 m distance to the load

Fig. 9. Pressure below the surface versus depth at different times.

point B in 10 m distance from the load (Fig. 9(b)) the result is presented. As expected, the pore pressure rises very fast from zero (the boundary condition at the surface) to its maximum value and tends to a constant value. For later times this maximum value is smaller and shifted to larger depth. Remarkable is that at point B the largest pore pressure is reached not at $t = 0.1$ s as at point A but at $t = 0.5$ s. However, comparing the total values of the pore pressure in both figures a difference of factor six is observed. So, at point B the largest pore pressure values are achieved at later times but also at lower values. This is in accordance with physical considerations. After loading the half space at point A, it takes time until the disturbance is observed in 10 m distance and also the value is reduced.

5. Conclusions

A novel application of the convolution quadrature method to quasi-static problems in viscoelasticity and poroelasticity is presented. Following the procedure known from the corresponding dynamic boundary element formulations, a time-stepping boundary element formulation based on the Laplace transformed fundamental solutions and on a linear multi-step method is established. Hence, only the Laplace domain fundamental solutions are necessary which can be derived much easier than in time domain.

Numerical studies concerning spatial discretization show that the poroelastic boundary element formulation needs a much finer mesh than the viscoelastic formulation. Concerning temporal discretization it can be concluded that both presented formulations are not sensitive on the choice of the time step size. The time step size must only be small enough to dissolve the time history of the modeled physical problem. Finally, one example for the creep behavior and one example for the consolidation are presented to show that the proposed formulation reproduces the main physical effects of quasi-static viscoelasticity and quasi-static poroelasticity correctly.

Appendix A. Poroelastic fundamental solutions

In the following, the explicit expressions of the poroelastic quasi-static fundamental solutions in 3-d are given. A collection of all types of fundamental solutions caused by different loads for a quasi-static poroelastic modeled continuum can be found in [23].

The displacement and the pressure due to a single source in the solid are

$$\widehat{U}_{ij}^s = \frac{1}{4\pi} \left\{ \frac{K + \frac{7}{3}G + M\alpha^2}{2G(K + \frac{4}{3}G + M\alpha^2)} \frac{\delta_{ij}}{r} \right.$$

$$\left. + \frac{K + \frac{1}{3}G + M\alpha^2}{2G(K + \frac{4}{3}G + M\alpha^2)} \frac{r_{,i}r_{,j}}{r} + \frac{\kappa M^2 \alpha^2}{s(K + \frac{4}{3}G + M\alpha^2)^2} \right.$$

$$\left. \times \frac{1}{r^3} \left[\delta_{ij} [1 - (1 + \xi)e^{-\xi}] + r_{,i}r_{,j} [(3 + 3\xi + \xi^2)e^{-\xi} - 3] \right] \right\} \tag{A.1}$$

$$\widehat{P}_i^s = -\frac{M\alpha}{4\pi s(K + \frac{4}{3}G + M\alpha^2)} \frac{r_{,i}}{r^2} [1 - (1 + \xi)e^{-\xi}] \tag{A.2}$$

and due to a source in the fluid are

$$\widehat{U}_i^f = -\frac{M\alpha}{4\pi(K + \frac{4}{3}G + M\alpha^2)} \frac{r_{,i}}{r^2} [1 - (1 + \xi)e^{-\xi}] \tag{A.3}$$

$$\widehat{P}^f = \frac{1}{4\pi\kappa} \frac{1}{r} e^{-\xi} \tag{A.4}$$

with $\xi = r\sqrt{\frac{s(K + \frac{4}{3}G + M\alpha^2)}{M\kappa(K + \frac{4}{3}G)}}$.

During derivation of the boundary integral equation from the weighted residual statement two integrations by part have to be performed. For convenience and also with a physical interpretation of an 'adjoint' traction or flux the following abbreviations are introduced

$$\widehat{T}_{ij}^s = \left[\left(\left(K - \frac{2}{3}G \right) \widehat{U}_{kj,k}^s + s\alpha\widehat{P}_j^s \right) \delta_{i\ell} + G \left(\widehat{U}_{ij,\ell}^s + \widehat{U}_{\ell j,i}^s \right) \right] n_\ell \tag{A.5a}$$

$$\widehat{Q}_j^s = \kappa\widehat{P}_{j,i}^s n_i \tag{A.5b}$$

$$\widehat{T}_i^f = \left[\left(\left(K - \frac{2}{3}G \right) \widehat{U}_{k,k}^f + s\alpha\widehat{P}^f \right) \delta_{i\ell} + G \left(\widehat{U}_{i,\ell}^f + \widehat{U}_{\ell,i}^s \right) \right] n_\ell \tag{A.5c}$$

$$\widehat{Q}^f = \kappa\widehat{P}_{,i}^f n_i. \tag{A.5d}$$

The explicit expression of these 'adjoint' tractions and fluxes are

$$\widehat{T}_{ij}^s = \frac{1}{4\pi(K + \frac{4}{3}G + M\alpha^2)} \frac{1}{r^2} \left[G(n_i r_{,j} - n_j r_{,i} - \delta_{ij} r_{,n}) \right.$$

$$\left. -3 \left(K + \frac{1}{3}G + M\alpha^2 \right) r_{,i}r_{,j}r_{,n} \right]$$

$$+ \frac{2GM^2\alpha^2\kappa}{4\pi s(K + \frac{4}{3}G + M\alpha^2)^2} \frac{1}{r^4}$$

$$\times \left[(\delta_{ij} r_{,n} + n_j r_{,i}) [(\xi^2 + 3\xi + 3)e^{-\xi} - 3] \right.$$

$$+ n_i r_{,j} [(\xi^3 + 2\xi^2 + 3\xi + 3)e^{-\xi} - 3]$$

$$\left. + r_{,i} r_{,j} r_{,n} [15 - (\xi^3 + 6\xi^2 + 15\xi + 15)e^{-\xi}] \right] \tag{A.6a}$$

$$\widehat{T}_i^f = \frac{2GM\alpha}{4\pi(K + \frac{4}{3}G + M\alpha^2)} \frac{1}{r^3} \left\{ n_i [(1 + \xi + \xi^2)e^{-\xi} - 1] \right.$$

$$\left. + r_{,i} r_{,n} [3 - (3 + 3\xi + \xi^2)e^{-\xi}] \right\} \tag{A.6b}$$

$$\widehat{Q}_j^s = \frac{M\alpha\kappa}{4\pi s\left(K + \frac{4}{3}G + M\alpha^2\right)} \frac{1}{r^3} \left\{ n_j\left[(1 + \xi)e^{-\xi} - 1\right] \right.$$
$$\left. + r_{,j}r_{,n}\left[3 - (3 + 3\xi + \xi^2)e^{-\xi}\right] \right\} \tag{A.6c}$$

$$\widehat{Q}^f = -\frac{1}{4\pi} \frac{r_{,n}}{r^2}(1 + \xi)e^{-\xi}. \tag{A.6d}$$

Note that $r_{,n} = r_{,k}n_k$ denotes the normal derivative.

Appendix B. Convolution quadrature method

The 'convolution quadrature method' developed by Lubich numerically approximates a convolution integral for $n = 0, 1, \ldots, N$

$$y(t) = \int_0^t f(t - \tau)g(\tau)\mathrm{d}\tau \rightarrow y(n\Delta t)$$
$$= \sum_{k=0}^n \omega_{n-k}(\Delta t)g(k\Delta t), \tag{B.1}$$

by a quadrature rule whose weights are determined by the Laplace transformed function $\hat{f}$ and a linear multi-step method. This method was originally published in [3] and [4]. Application to the boundary element method may be found in [2]. Here, a brief overview of the method is given.

In formula (B.1), the time t is divided in N equal steps Δt. The weights $\omega_n(\Delta t)$ are the coefficients of the power series

$$\hat{f}\left(\frac{\gamma(z)}{\Delta t}\right) = \sum_{n=0}^{\infty} \omega_n(\Delta t)z^n \tag{B.2}$$

with the complex variable z. The coefficients of a power series are usually calculated with Cauchy's integral formula. After a polar coordinate transformation, this integral is approximated by a trapezoidal rule with L equal steps $\frac{2\pi}{L}$. This leads to

$$\omega_n(\Delta t) = \frac{1}{2\pi\mathrm{i}} \int_{|z|=R} \hat{f}\left(\frac{\gamma(z)}{\Delta t}\right) z^{-n-1}\mathrm{d}z$$
$$\approx \frac{\mathscr{R}^{-n}}{L} \sum_{\ell=0}^{L-1} \hat{f}\left(\frac{\gamma\mathscr{R}e^{\mathrm{i}\ell\frac{2\pi}{L}}}{\Delta t}\right) e^{-\mathrm{i}n\ell\frac{2\pi}{L}}, \tag{B.3}$$

where $\mathscr{R}$ is the radius of a circle in the domain of analyticity of $\hat{f}(z)$.

The function $\gamma(z)$ is the quotient of the characteristic polynomials of the underlying multi-step method, e.g., for a BDF 2, $\gamma(z) = 3/2 - 2z + 1/2z^2$. The used linear multi-step method must be $A(\alpha)$-stable and stable at infinity [4]. Experience shows that the BDF 2 is the best choice [7]. Therefore, it is used in all calculations in this paper.

If one assumes that the values of $\hat{f}(z)$ in (B.3) are computed with an error bounded by ϵ, then the choice $L = N$ and $\mathscr{R}^N = \sqrt{\epsilon}$ yields an error in ω_n of size $\mathrm{O}(\sqrt{\epsilon})$ [3]. Several tests conducted by the first author lead to the conclusion that the parameter $\epsilon = 10^{-10}$ is the best choice for the kind of functions dealt with in this paper [1]. The assumption $L = N$ leads to a order of complexity $\mathrm{O}(N^2)$ for calculating the N coefficients $\omega_n(\Delta t)$. Due to the exponential function at the end of formula (B.3) this can be reduced to $\mathrm{O}(N\log N)$ using the technique of the Fast Fourier Transformation (FFT).

References

[1] Schanz M, Antes H. Application of 'operational quadrature methods' in time domain boundary element methods. Meccanica 1997;32:179–86.

[2] Schanz M, Antes H. A new visco- and elastodynamic time domain boundary element formulation. Comput Mech 1997;20:452–9.

[3] Lubich C. Convolution quadrature and discretized operational calculus. I. Numer Math 1988;52:129–45.

[4] Lubich C. Convolution quadrature and discretized operational calculus. II. Numer Math 1988;52:413–25.

[5] Schanz M. Wave propagation in viscoelastic and poroelastic continua: a boundary element approach. In: Lecture notes in applied mechanics. Berlin, Heidelberg, New York: Springer-Verlag; 2001.

[6] Abreu AI, Carrer JAM, Mansur WJ. Scalar wave propagation in 2D: a BEM formulation based on the operational quadrature method. Eng Anal Boundary Elem 2003;27:101–5.

[7] Schanz M. A boundary element formulation in time domain for viscoelastic solids. Commun Numer Methods Eng 1999;15:799–809.

[8] Schanz M. Application of 3-d boundary element formulation to wave propagation in poroelastic solids. Eng Anal Boundary Elem 2001;25:363–76.

[9] Zhang Ch, Sladek J, Sladek V. Effects of material gradients on transient dynamic mode-III stress intensity factors in a FGM. Int J Solids Struct 2003;40:5251–70.

[10] Antes H, Schanz M, Alvermann S. Dynamic analyses of frames by integral equations for bars and Timoshenko beams. J Sound Vib 2004;276:807–36.

[11] Zhang Ch. Transient elastodynamic antiplane crack analysis in anisotropic solids. Int J Solids Struct 2000;37:6107–30.

[12] Zhang Ch. Transient dynamic response of a cracked piezoelectric solid under impact loading. In: Wendland W, Efendiev M, editors. Analysis and simulation of multifield problems. Lecture notes in applied and computational mechanics, vol. 12. Berlin, Heidelberg, New York: Springer-Verlag; 2003. p. 247–53.

[13] Sim WJ, Kwak BM. Linear viscoelastic analysis in time domain by boundary element method. Comput Struct 1988;29:531–9.

[14] Carini A, Diligenti M, Maier G. Boundary integral equation analysis in linear viscoelasticity: variational and saddle point formulations. Comput Mech 1991;8:87–98.

[15] Dargush GF, Banerjee PK. A time domain boundary element method for poroelasticity. Int J Numer Methods Eng 1989;28:2423–49.

[16] Lee SS. Boundary element analysis of linear viscoelastic problems using realistic relaxation functions. Comput Struct 1995;55:1027–36.

[17] Gaul L. The influence of damping on waves and vibrations. Mech Syst Signal Process 1999;13:1–30.

[18] Biot MA. General theory of three-dimensional consolidation. J Appl Phys 1941;12:155–64.

[19] de Boer R. Theory of porous media. Berlin: Springer-Verlag; 2000.

[20] Schanz M, Diebels S. A comparative study of Biot's theory and the linear Theory of Porous Media for wave propagation problems. Acta Mech 2003;161:213–35.

[21] Christensen RM. Theory of viscoelasticity. New York: Academic Press, 1971.

[22] Badmus T, Cheng AH-D, Grilli S. A Laplace-transform based three-dimensional BEM for poroelasticity. Int J Numer Methods Eng 1993;36:67–85.

[23] Cheng AH-D, Detournay E. On singular integral equations and fundamental solutions of poroelasticity. Int J Solids Struct 1998;35:4521–55.

[24] Detournay E, Cheng AH-D. Fundamentals of poroelasticity. Comprehensive rock engineering: principles, practice and projects, vol. II. Pergamon Press; 1993. p. 113–71. [Chapter 5].

[25] Bagley RL, Torvik PJ. On the fractional calculus model of viscoelastic behaviour. J Rheol 1986;30:133–55.

[26] Gaul L, Schanz M. Dynamics of viscoelastic solids treated by boundary element approaches in time domain. Eur J Mech A—Solids 1994;13:43–59.

[27] Bonnet G. Basic singular solutions for a poroelastic medium in the dynamic range. J Acoust Soc Am 1987;82: 1758–62.

[28] Gurtin ME, Sternberg E. On the linear theory of viscoelasticity. Arch Rational Mech Anal 1962;11:291–356.

[29] Cheng AH-D, Ligget JA. Boundary integral equation method for linear porous-elasticity with applications to soil consilidation. Int J Numer Methods Eng 1984;20: 255–78.

[30] Mantič V. A new formula for the *C*-matrix in the somigliana identity. J Elasticity 1993;33:191–201.

[31] Guiggiani M, Gigante A. A general algorithm for multidimensional cauchy principal value integrals in the boundary element method. J Appl Mech, ASME 1990;57: 906–15.

[32] Domínguez J. Boundary elements in dynamics. Southampton: Computational Mechanics Publication; 1993.

[33] Kim YK, Kingsbury HB. Dynamic characterization of poroelastic materials. Exp Mech 1979;19:252–8.